HHS Public Access

Author manuscript

Biochemistry. Author manuscript; available in PMC 2019 May 15.

Published in final edited form as:

Biochemistry. 2018 May 15; 57(19): 2846–2856. doi:10.1021/acs.biochem.8b00309.

Initial Biochemical and Functional Evaluation of Murine Calprotectin Reveals Ca(II)-Dependence and Its Ability to Chelate Multiple Nutrient Transition Metal Ions

Rose C. Hadley, **Yu Gu**, and **Elizabeth M. Nolan***

Department of Chemistry, Massachusetts Institute of Technology, Cambridge, MA 02139, USA

Abstract

Calprotectin (CP) is an abundant host-defense protein that contributes to the metal-withholding innate immune response by sequestering nutrient metal ions from microbial pathogens in the extracellular space. Over the past decade, murine models of infectious disease have advanced understanding of the physiological functions of CP and its ability to compete with microbes for essential metal nutrients. Despite this extensive work, murine CP (mCP) has not been biochemically evaluated, and structural and biophysical understanding of CP is currently limited to the human orthologue. We present the reconstitution, purification, and characterization of mCP as well as the cysteine-null variant mCP-Ser. Apo mCP is a mS100A8/mS100A9 heterodimer and Ca(II) binding causes two heterodimers to self-associate and form a heterotetramer. Initial metal-depletion studies demonstrate that mCP depletes multiple first-row transition metal ions, including Mn, Fe, Ni, Cu and Zn, from complex microbial growth medium, indicating that mCP binds multiple nutrient metals with high affinity. Moreover, antibacterial activity assays show that mCP inhibits the growth of a variety of bacterial species. The metal-depletion and antibacterial activity studies also provide evidence that Ca(II) ions enhance these functional properties of mCP. This contribution provides the groundwork for understanding the similarities and differences between the human and murine orthologues of CP, and for further elucidation of its biological coordination chemistry.

Graphical Abstract

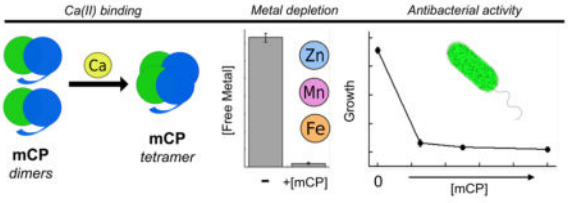

*Corresponding author: lnolan@mit.edu, Phone: 617-452-2495.

Supporting information

Description of the synthetic gene design, Tables S1–S5, and Figures S1–S4. This material is available free of charge via the Internet at http://pubs.acs.org.

Introduction

S100 proteins serve important and diverse functions in the life processes of vertebrates, and share some distinguishing features.[1] These proteins are predominantly α-helical, have a propensity to self-associate and typically form homodimers, contain Ca(II)-binding EF-hand domains, and possess varying capacities for coordinating Ca(II) and divalent transition metal ions.[1, 2] Several S100 proteins, including human S100A7 (psoriasin), human S100A12, and the S100A8/S100A9 heterooligomer calprotectin (CP), contribute to the metal-withholding innate immune response and exhibit antimicrobial activity attributed to their ability to sequester transition metal ions from microbial pathogens in the extracellular space.[3–5]

CP is the most thoroughly evaluated metal-sequestering S100 protein. Both humans and mice express CP in epithelial and white blood cells, and our current understanding of its contributions to metal homeostasis and the innate immune response results from early clinical investigations and *ex vivo* analyses of human specimens, murine model studies of infectious disease, and chemical and biological studies of the human orthologue obtained by recombinant protein expression.[5] Murine infection model studies have leveraged *S100A9*$^{-/-}$ knockout mice, which are effectively CP deficient,[6] to provide insight into the role of murine CP (mCP) during acute bacterial and fungal infections. For instance, seminal studies using a *Staphylococcus aureus* infection model in wild-type and *S100A9*$^{-/-}$ mice revealed that CP contributes to manganese withholding.[7] Since this work, *S100A9*$^{-/-}$ mice have been used to investigate the interplay between CP and a variety of microbial pathogens that include *Salmonella enterica* serovar Typhimurium,[8, 9] *Acinetobacter baumannii*,[10–13] *Streptococcus pneumoniae,*[14] *Helicobacter pylori,*[15] *Aspergillus fumigatus,*[16] and *Candida albicans.*[17, 18] Taken together, these studies illuminate that the contributions of mCP to metal availability and the host/pathogen interaction are varied and context dependent. For example, some pathogens like *Salmonella* and *S. pneumoniae* appear to benefit from mCP-mediated metal limitation,[8, 9, 14] and recent work indicates that the role of mCP in metal-withholding can be organ-specific.[19] In addition, mCP has been shown to modulate the composition of polymicrobial communities *in vivo.*[20]

The working model for the extracellular metal-sequestering function of CP begins with its release from white blood cells, especially neutrophils recruited to an infection site, and epithelial cells. Once in the extracellular space, CP competes with invading microbial pathogens for available transition metal nutrients. Studies of recombinant human CP (hCP) have informed our understanding of its competition with microbes for metal nutrients, including the molecular basis for this process. hCP is a heterooligomer of two S100 polypeptides, hS100A8 (α subunit, 10.8 kDa) and hS100A9 (β subunit, 13.2 kDa). Like other S100 polypeptides, each subunit harbors two Ca(II)-binding EF-hand domains.[2, 21] The C-terminal EF-hands, described as “canonical,” bind Ca(II) in a heptadentate coordination geometry. The N-terminal EF-hands are considered “non-canonical” and bind Ca(II) with lower coordination number and lower affinity. Apo hCP, which we define as the species that does not have Ca(II) ions or transition metal ions bound, is a hS100A8/hS100A9 heterodimer.[22] Each heterodimer unit harbors two sites for transition metals that form at the hS100A8/hS100A9 interface and are comprised of metal-chelating residues from both subunits.[21, 23] Site 1 is a His_3Asp motif formed by His83 and His87 of hS100A8, and His20

and Asp30 of hS100A9. Site 2 is an unusual His_6 motif formed by His17 and His27 of hS100A8, and His91, His95, His103 and His105 of hS100A9.[24, 25] Binding of Ca(II) ions at the EF-hands or a transition metal ion at the His_6 site causes self-association of two hCP heterodimers to form a heterotetramer.[26–29] The Ca(II)-bound heterotetramer exhibits enhanced transition metal affinities relative to the Ca(II)-free heterodimer, and this feature indicates that hCP morphs into its metal-sequestering form in the extracellular space where Ca(II) ion concentrations are ≈2 mM.[23, 30, 31] Along similar lines, Ca(II) ions enhance the antimicrobial activity of hCP against a variety of bacterial species.[7, 23, 32] Its growth inhibitory activity was originally attributed to Zn(II) and then also Mn(II) sequestration.[7, 33, 34] More recent work has demonstrated additional Fe(II)-, Ni(II)-, and Cu(II)-sequestering properties of hCP, and affords a model of functional versatility in which hCP has the capacity to bind and entrap multiple divalent nutrient metal ions.[18, 31, 35]

This discussion highlights that classical biochemical and microbiology studies have focused on the human orthologue. Accordingly, results from biochemical and functional investigations of hCP are used to inform studies in murine model systems and vice versa with the apparent presumption that hCP and mCP behave similarly. To the best of our knowledge, little is known about the biochemical and biophysical properties of mCP, which presents a limitation in our current appreciation of the similarities and differences of CP orthologues. Although procedures to obtain recombinant mS100A8 and recombinant mS100A9 have been reported,[36, 37] we are unaware of any work describing robust reconstitution of the mCP heterooligomer. Reports related to mCP include early investigations demonstrating the isolation of mS100A8 (originally named CP-10)[38] and mS100A9 (originally named murine MRP14)[39] from activated spleen cells. In the latter study, mS100A8 and mS100A9 were reported to co-purify by ion-exchange chromatography.[39] Moreover, analysis of murine abscess fluid revealed the presence of mS100A8/mS100A9 complexes as well as unassociated mS100A8 and mS100A9 species.[40] This study also reported that the abscesses contained high levels of mS100A8 (≈8 mg/mL, ≈780 μM) and mS100A9 (≈6 mg/mL, ≈460 μM).[40] Lastly, murine model systems are highly informative, but there are some caveats to their applicability to the host/pathogen interaction in humans because of inherent differences between the murine and human immune systems.[41] For these reasons, we concluded that mCP warrants biochemical consideration and that studies of this protein will improve our understanding of CP in metal withholding and other biological phenomena.

Amino acid sequence alignment provides a first point of comparison between human and murine CP (Figure 1). The human and murine forms of S100A8 share 52 identical amino acid residues (56% identity) and 15 similar amino acid residues (72% similarity), and the corresponding S100A9 peptides share 66 identical amino acid residues (57% identity) and 10 similar amino acids (66% similarity). The residues that comprise the His_3Asp and His_6 metal-binding sites of hCP are conserved in the murine polypeptides, suggesting that mCP employs the same metal-binding sites as hCP. Moreover, the Ca(II)-binding loops of the human and murine S100A8 and S100A9 subunits possess similar residues. Nevertheless, inspection of the amino acid sequences reveals several intriguing differences between the human and murine polypeptides. In particular, the C-terminus of mS100A8 lacks the EESH motif of hS100A8, and the S100A9 C-terminal tail regions exhibit low sequence identity.

The hS100A9 C-terminal tail is an important contributor to the His_6 metal-binding site because it provides two His residues that complete the octahedral coordination sphere and encapsulates the bound M(II) ion (M = Fe, Mn, Ni, Zn) at this site.[24, 25, 31, 35, 42, 43] Curiously, the mS100A9 tail contains an HxHxH motif (residues 103-107) rather than the HHH motif (residues 103-105) of hS100A9. We also note that hS100A8 and mS100A8 each contain one conserved Cys residue at position 42. In contrast, the quantity and locations of the Cys residues in hS100A9 and mS100A9 differ. Whereas hS100A9 contains one Cys residue at position 3, which is located before an alternative translation start site at position 5, mS100A9 contains three Cys residues at positions 80, 91 and 111.

In this work, we present initial biochemical and functional characterization of mCP and the cysteine-null variant mCP-Ser. The results demonstrate that apo mCP is a heterodimer and that the protein tetramerizes in the presence of Ca(II), binds various first-row transition metal ions, and displays broad-spectrum antibacterial activity. These properties are reminiscent of hCP; however, this study also reveals several differences between the human and murine orthologues. In particular, mCP appears to be less responsive to Ca(II) ions than hCP. Overall, this work provides a foundation for further investigations of mCP and informs prior and future studies of mCP in murine models of disease.

Experimental Section

General Materials and Methods

All chemicals were acquired from commercial suppliers and used as received. All solutions were prepared using Milli-Q water (18.2 MΩ·cm). All buffer solutions were filtered (0.2 μm) before use. Stock solutions (1 M, 100 mL) of Ca(II) ($CaCl_2 \cdot 2H_2O$, Sigma, >99.0%) were prepared in acid-washed volumetric glassware and transferred to polypropylene tubes for storage. Working solutions of Ca(II) were prepared immediately before use by diluting the 1-M stock solution in Milli-Q water. ULTROL grade HEPES (Calbiochem) and BioXtra NaCl (>99.5%) were used to prepare buffers for analytical SEC to minimize metal ion contamination from the buffer. The hCP-Ser heterodimer was prepared as previously described.[23] Protein aliquots were thawed only once, immediately prior to use. All concentrations were determined using calculated extinction coefficients (https://web.expasy.org/protparam/), and all reported concentration are for heterodimers or homodimers: murine S100A8/S100A9 heterodimer (ε_{280} = 5,960 $M^{-1}cm^{-1}$), human S100A8/S100A9 heterodimer (ε_{280} = 18,450 $M^{-1}cm^{-1}$).

Sub-cloning of mS100A8 and mS100A9

Synthetic genes containing the nucleotide sequences for mS100A8, mS100A9, and mS100A9(C80S)(C91S)(C111S) were codon-optimized for *Escherichia coli* expression, synthesized, and ligated into the *Nde*I and *Xho*I restriction sites of pET41a by DNA2.0 (Supporting Information). Each plasmid was transformed into chemically competent *E. coli* TOP10, isolated using a miniprep kit (Qiagen), and analyzed by DNA sequencing (Quintara Biosciences). The pET41a-*mS100A8(C42S)* plasmid was obtained by site-directed mutagenesis as described below. For protein expression, each plasmid was transformed into chemically competent *E. coli* BL21(DE3). Single colonies were grown to saturation in LB

medium containing 50 μg/mL kanamycin (37 °C with agitation). Freezer stocks were prepared by diluting the culture 1:1 with 50% v/v glycerol in filter-sterilized Milli-Q water and stored at −80 °C.

Site-directed Mutagenesis

The oligonucleotide primers employed to prepare the mS100A8(C42S) variant by site-directed mutagenesis were synthesized by Integrated DNA Technologies (Coralville, IA). pET41a-*mS100A8(C42S)* was prepared using pET41a-*mS100A8* as a template and a modified Quick-Change site-directed mutagenesis protocol. The forward primer 5′-GATGGTTACCACGGAGAGCCCGCAGTTCGTGCAG-3′ and the reverse primer 5′-CTGCACGAACTGCGGGCTCTCCGTGGTAACCATC-3′ (mutation sites underlined) were used in PCR reactions with Pfu Turbo DNA polymerase. The PCR protocol was 95 °C for 30 sec; 95 °C for 30 sec, 60 °C for 1 min, 68 °C for 12 min (25x); 4 °C hold temperature. *Dpn*I (New England Biolabs) was used to degrade the template plasmid by adding a 0.75-μL aliquot to the sample, and incubating the sample at 37 °C for 3 h. A supplemental 0.75 μL aliquot of *DpnI* was added at 1.5 h into the incubation. The resulting DNA was transformed into chemically-competent *E. coli* TOP10 and the cells were plated on agar containing 50 μg/mL kanamycin. Single colonies were inoculated into LB (5 mL, 50 μg/mL kanamycin) and grown overnight, and plasmids were obtained using a miniprep kit (Qiagen). The plasmids were analyzed by DNA sequencing (Quintara Biosciences) to confirm the presence of the desired mutation and then transformed into chemically competent *E. coli* BL21(DE3) for protein overexpression.

Overexpression of mS100A8 and mS100A9

For protein overexpression, overnight cultures in LB with 50 μg/mL kanamycin were inoculated from freezer stocks and grown to saturation (37 °C with agitation, ≈16 h) and used to inoculate 1 L of LB with 50 μg/mL kanamycin (1:100 dilution). These cultures were grown at 37 °C with shaking at 150 rpm, induced with 100 μM IPTG at OD_{600} ≈0.6–0.7, and then incubated for an additional ≈3.5–4 h at 37 °C with shaking at 150 rpm and pelleted by centrifugation (3,000 rpm, 15 min, 4 °C). The pellets were transferred to polypropylene tubes, flash frozen in liquid N_2, and stored at −80 °C. Typical cell pellets weighed ≈2–3 g/L culture. This overexpression procedure resulted in mS100A8 in the insoluble fraction and mS100A9 in the soluble fraction following cell lysis.

Reconstitution and Purification of mCP and mCP-Ser

All steps were performed on ice or in a 4 °C room. For reconstitution and purification of the mCP heterodimer, one mS100A8 and one mS100A9 cell pellet, each from a 1-L overexpression, were thawed on ice and each pellet was suspended in 30 mL lysis buffer A (50 mM Tris, 100 mM NaCl, 1 mM EDTA, 0.5% Triton X-100, pH 8.0) supplemented with 5 mM DTT and 1 mM PMSF (from a freshly prepared ≈1 mL solution in ethanol) immediately before use. The resuspended cell pellets were combined and sonicated (2.5 min, 30 sec on, 10 sec off, 40% amplitude) in a steel beaker on ice. The cell lysate was then clarified by centrifugation (14,000 rpm, 10 min, 4 °C). The supernatant, which contained soluble mS100A9, was transferred to a 250-mL glass beaker on ice and the cell pellets, which contained insoluble mS100A8, were combined in 60 mL of lysis buffer A and

subjected to a second round of resuspension, sonication, and centrifugation. The resulting pellets containing mS100A8 were stored on ice, and the combined supernatant containing mS100A9 was treated with 60% ammonium sulfate to precipitate contaminating proteins (rapid stirring, ≈1 h, 4 °C). The resulting mixture was centrifuged (14,000 rpm, 20 min, 4 °C) and filtered. The filtered supernatant was collected and treated with 100% ammonium sulfate to precipitate mS100A9 (rapid stirring, ≈1 h, 4 °C). The mixture was centrifuged (14,000 rpm, 20 min, 4 °C) and filtered, and the supernatant discarded, which afforded cell pellets containing mS100A9. At this point, the mS100A8 and mS100A9 cell pellets were combined and resuspended in 100 mL lysis buffer B (50 mM Tris, 100 mM NaCl, 4 M Gu-HCl, pH 8.0) supplemented with 5 mM DTT and the resulting mixture was sonicated (5 min, 30 sec on, 10 sec off, 40% amplitude) and centrifuged (14,000 rpm, 10 min, 4°C). The resulting supernatant containing denatured mS100A8 and denatured mS100A9 was transferred to a dialysis bag (SpectraPor, 3,500 MWCO) and dialyzed against MonoQ buffer A (20 mM HEPES, pH 8.0) supplemented with 5 mM DTT (4 L, > 12 h, 3x, 4 °C). DTT powder was added to each dialysis buffer immediately before use.

Purification of the mCP heterodimer was performed by anion exchange chromatography and SEC. After dialysis, the protein solution was centrifuged (14,000 rpm, 10 min, 4 °C), filtered (0.2 μm) and loaded onto a pre-equilibrated MonoQ 10/100 column (GE Life Sciences) using a Superloop (150 mL, GE Life Sciences). The anion exchange buffers were MonoQ buffer A (20 mM HEPES, pH 8.0) and MonoQ buffer B (20 mM HEPES, 1 M NaCl, pH 8.0), and both buffers were supplemented with 5 mM DTT immediately before use. The protein was eluted using a gradient of 0–15% B over 15 column volumes of MonoQ buffer B. The fractions containing mCP were combined, concentrated to ≈10 mL by spin filtration (Amicon, 10 kDa MWCO) and loaded onto a pre-equilibrated HiLoad 26/600 Superdex S75 column (GE Life Sciences) using S75 buffer (20 mM HEPES, 100 mM NaCl, pH 8.0) containing 5 mM DTT. The protein was eluted over 1 column volume and dialyzed against 20 mM HEPES, 100 mM NaCl, pH 8.0, 5 mM DTT that contained ≈10 g Chelex resin (Biorad), typically overnight (>12 h) at 4°C before being filtered (0.2 μm) and concentrated by spin filtration (Amicon, 15-mL filter, 10 kDa MWCO), flash frozen in aliquots (50 μL), and stored at −80 °C. Typical yields of mCP were ≈45 mg/2 L culture (1 L from each subunit overexpression). The mCP-Ser variant was prepared using the same procedures except that DTT was omitted from all buffers. Typical yields of mCP-Ser were ≈16 mg/2 L of culture.

Electrospray Ionization Mass Spectrometry (ESI-MS)

A denaturing protocol was employed to analyze mCP, mCP-Ser, mS100A8 and mS100A9 by LC-MS. An Agilent 1260 series LC system outfitted with an Agilent Jetstream ESI source and an Agilent Poroshell 300SB-C18 column (5-μm pore size) was used for all analyses. Each protein was diluted in Milli-Q water to provide a final concentration of ≈5 μM. A 5-μL protein sample was injected onto the column, and the mS100A8 and mS100A9 subunits were eluted using a gradient of 10–90% B over 20 min with a flow rate of 0.2 mL/min (solvent A: 0.1% formic acid in water; solvent B: 0.1% formic acid in acetonitrile). The spectra were deconvoluted using the maximum entropy algorithm in the MassHunter software (Agilent).

Circular Dichroism Spectroscopy

A Jasco J-1500 circular dichroism (CD) spectrometer housed in the Biophysical Instrumentation Facility at MIT was used for all measurements. Proteins were buffer-exchanged into CD buffer (1 mM Tris-HCl, pH 7.5). The buffer was supplemented with 1 mM DTT for all proteins except for mCP-Ser. For samples that contained Ca(II), an aliquot from a 1-M Ca(II) stock solution was added to the protein solution to afford a final Ca(II) concentration of 3 mM. Each sample (10 μM protein, 300 μL) was transferred to a nitric acid-washed Hellma quartz cuvette (1-mm path length). Spectra were recorded from 195 to 260 nm using continuous scan mode (50 nm/min) and 1 nm bandwidth. All data represent averages of three replicate baseline-subtracted scans, where the baseline was obtained from a sample of CD buffer. For thermal denaturation experiments, the temperature was increased from 25–95 °C, at 1-°C intervals, and the CD intensity was recorded at 222 nm. Each thermal denaturation experiment was repeated on three independent samples and data from one representative experiment are shown.

Analytical Size Exclusion Chromatography

An ÄKTA Purifier FPLC system housed in a cold room (4 °C) and outfitted with a Superdex 75 10/300 GL SEC column was used for all analytical SEC. The running buffer was 75 mM HEPES, pH 7.0, 100 mM NaCl, 200 μM TCEP containing 0, 2, 5, 10 or 25 mM Ca(II). The column was calibrated with blue dextran and a low-molecular-weight protein mixture (GE Healthcare Life Sciences) consisting of ribonuclease A (13.7 kDa), carbonic anhydrase (29 kDa), ovalbumin (44 kDa), and conalbumin (75 kDa) prior to use. Proteins were buffer-exchanged (3x) into the running buffer using an Amicon spin filter (0.5 mL, 10 kDa MWCO). Samples (100 μM, 300 μL) were prepared and loaded into a 100-μL injection loop, and the FPLC system was programmed to inject 500 μL of sample onto the column. The samples were eluted over one column volume at a flow rate of 0.5 mL/min. At least two independent replicates were performed for each experiment, and representative data from one experiment are shown.

Metal Depletion Assay

The assay protocols were adapted from a reported procedure.[31] Antimicrobial activity (AMA) buffer (20 mM Tris-HCl, pH 7.5, 100 mM NaCl) was sterile filtered (0.22 μm) into sterile 50-mL polypropylene tubes (VWR). AMA media (62:38 v/v ratio of AMA buffer and TSB; ± 3 mM BME, ± 2 mM Ca(II)) was then prepared. Proteins were buffer-exchanged into AMA buffer using 0.5-mL Amicon spin filters (10 kDa MWCO). Aliquots (1 mL) of AMA media were placed into pre-sterilized 1.7-mL microcentrifuge tubes (VWR). Protein was then added from a concentrated stock solution to afford a final concentration of 250 μg/mL. The total volume change upon protein addition was ≤2%. The tubes were closed and incubated at 30 °C (150 rpm, 20 h). Subsequently, the samples were transferred by pipette to sterile 4-mL Amicon spin filters (10 kDa MWCO) and centrifuged (3700 rpm, 30 min, 4 °C). Samples for ICP-MS analyses were prepared by combining 700 μL of the filtrate with 700 μL of ≈3% nitric acid, and spiking the resulting mixture with 28 μL (2 ppb) of Tb internal standard (Agilent).

ICP-MS

Metal ion concentrations were quantified by using an Agilent 7900 ICP-MS housed in the Center for Environmental Health Sciences Bioanalytical Core Facility at MIT. The instrument was operated in helium mode. The instrument was calibrated before each analysis session using a series of five serially diluted (1:10 in ≈3% nitric acid) samples of the Environmental Calibration Standard (Agilent, part # 5183-4688) as well as a nitric acid only standard. Each standard and sample was spiked with 2 ppb of the Terbium Internal Standard (Agilent, part # 5190-8590).

Antimicrobial Activity Assays

Assays were performed by adapting a reported protocol.[23] Cultures were grown in TSB without dextrose for *Escherichia coli* CFT073, *Acinetobacter baumannii* ATCC 17691, and *Staphylococcus aureus* USA300 JE2. *Listeria monocytogenes* ATCC 19115 and *Staphylococcus epidermidis* NRS101 were grown in BHI broth, and *Lactobacillus plantarum* WCFS1 was grown in MRS medium. Protein aliquots were buffer-exchanged into AMA buffer (20 mM Tris-HCl, pH 7.5, 100 mM NaCl) using a 0.5-mL Amicon spin filter (Millipore, 10-kDa MWCO). The protein was then diluted in AMA media (62:38 v/v ratio of 20 mM Tris-HCl pH 7.5, 100 mM NaCl and TSB, BHI or MRS; ± 3 mM BME, ± 2 mM Ca(II)) to afford 10x stock solutions (1 mg/mL – 313 μg/mL). Overnight cultures were prepared from single colonies and grown in 5 mL of TSB or BHI (37 °C, ≈16–20 h). The overnight cultures were diluted 1:100 into fresh TSB, BHI, or MRS and grown at 37 °C until the OD_{600} reached ≈0.6. Each culture was then diluted 1:500 into AMA media and the assays were immediately set up in 96-well plates (Corning) using 90 μL of the diluted bacterial culture and 10 μL of the protein stocks (or no-protein control). Each condition was performed in triplicate in the assay plate. The plates were wrapped in moist paper towels and plastic wrap and incubated with shaking at 150 rpm at 37 °C. The OD_{600} was measured at 8 and 20 h. Three independent replicates of each assay were performed and the resulting averages and standard deviation are reported.

Results

Purification of mCP and mCP-Ser

Guided by procedures to obtain the hS100A8 and hS100A9 subunits of hCP,[23] the mCP subunits mS100A8 and mS100A9 were overexpressed separately in *E. coli* BL21(DE3) at 37 °C. SDS-PAGE of post-induction samples identified the mS100A8 subunit in the insoluble fraction, as observed for hS100A8 and hS100A9 expressed under the same conditions.[23] In contrast, the mS100A9 subunit was only identified in the soluble fraction. Thus, we took the different solubilities of mS100A8 and mS100A9 into account during the development and optimization of a purification procedure. We found that it was most efficient to combine the mS100A8 and mS100A9 cell pellets and lyse this mixture. Following centrifugation, the soluble fraction containing mS100A9 was decanted and stored on ice. The insoluble fraction, which contained mS100A8, was subjected to an additional round of resuspension, lysis and centrifugation to remove contaminating biomolecules. The soluble fraction containing mS100A9 was then treated with 60% ammonium sulfate to precipitate contaminating proteins, which were removed by centrifugation and filtration. The

resulting supernatant was treated with 100% ammonium sulfate to precipitate mS100A9, which was pelleted by centrifugation. The resulting pellets containing mS100A9 were combined with the mS100A8 pellets in a solubilizing buffer containing 4 M GuHCl, and, following sonication and centrifugation, the soluble denatured sample was dialyzed against HEPES buffer to allow protein folding to occur. Anion exchange chromatography of the dialyzed sample and SDS-PAGE of the resulting fractions revealed that folding resulted in a mixture that predominantly contained mCP (evidenced by comparable quantities of mS100A8 and mS100A9) with some mS100A9 homodimer, which were separated by this chromatographic method. Subsequent gel filtration chromatography of the mCP-containing fractions and dialysis against Chelex resin afforded purified mCP heterodimer in yields of ≈45 mg from 2 L culture. mCP-Ser was purified in the same manner; however, lower yields of ≈16 mg from 2 L culture were repeatedly obtained for this variant. In general, the anion-exchange chromatograms for mCP-Ser indicated that greater amounts of mS100A9-Ser homodimer formed during folding compared to the amounts of mS100A9 observed during mCP preparations.

The purified proteins were evaluated by SDS-PAGE, mass spectrometry, and ICP-MS (Figure S1, Tables S1, S2). These analyses confirmed protein identity and indicated high purity by SDS-PAGE and negligible metal contamination. Moreover, CD spectroscopy (Figure S2, S2) and analytical SEC (Figure 3, Table S3) demonstrated that apo mCP and mCP-Ser were isolated as α-helical heterodimers as described further below.

mCP is α-Helical and Displays High Thermal Stability

The CD spectra of mCP and mCP-Ser displayed features characteristic of a predominantly α-helical protein in the presence and absence of Ca(II), as expected for S100 family members and consistent with the CD signatures of hCP and hCP-Ser (Figures 2, S2).[23] Thermal denaturation of 10 μM mCP at pH 7.5 afforded a melting temperature (T_m) of ≈76 °C that increased to ≈90 °C when 2 mM Ca(II) was added to the sample (Figure S3). mCP-Ser also displayed a Ca(II)-dependent increase in its T_m value from ≈63 °C to ≈77 °C in the absence and presence of 2 mM Ca(II), respectively. A comparison of the mCP and mCP-Ser data indicate that the Cys→Ser mutations that afford mCP-Ser destabilized the protein fold to thermal denaturation. The observed Ca(II) dependence for both proteins is in general agreement with reported thermal denaturation and differential scanning calorimetry studies of the human orthologue.[23, 28] For instance, the presence of excess Ca(II) ions caused the T_m value of CP-Ser to increase from 59 to 79 °C.[23]

mCP Exhibits Ca(II)-dependent Oligomerization

hCP exhibits Ca(II)-dependent oligomerization properties; the apo protein is a heterodimer and Ca(II) binding causes two heterodimers to self-associate and form a heterotetramer.[26–28] To evaluate whether mCP displays similar behavior, we investigated its oligomeric state in the absence and presence of Ca(II) ions using analytical SEC (Figure 3, Table S3). In the absence of added Ca(II) ions, mCP and mCP-Ser each exhibited an elution volume of ≈12.2 mL, which corresponds to a calculated molecular weight of 27 kDa and was assigned to the 23-kDa heterodimer. Next, we examined the elution profile of mCP and mCP-Ser in the presence of excess Ca(II) ions in the running buffer. At the highest Ca(II) concentration

examined (25 mM, 250 equivalents), each protein exhibited an elution volume of ≈11.4 mL, which corresponds to a calculated molecular weight of 38 kDa and was assigned to the 46-kDa heterotetramer. Thus, similar to hCP, Ca(II) binding to the EF-hands of the mCP heterodimer causes formation of heterotetramers. Nevertheless, the details of this self-association process appear to be markedly different for hCP and mCP. Our prior studies of hCP indicated that full conversion to the heterotetramer occurs when the protein is in the presence of ≈20 equivalents of Ca(II) ions.[23, 30, 31] The SEC results for mCP indicated that a mixture of heterodimers and heterotetramers exist under these conditions, and that >200 equivalents of Ca(II) are required for complete conversation to the heterotetramer.

mCP Depletes Multiple Transition Metals from Microbial Growth Media

Because amino acid sequence alignment indicates that the transition-metal-binding residues in hCP are conserved in mCP (Figure 1), we hypothesized that mCP exhibits similar coordination chemistry to hCP – i.e. His_3Asp and His_6 sites with similar metal selectivity. In our prior studies of metal chelation by hCP, we designed a simple assay to ascertain what metal ions the protein depletes from microbial growth media,[31] and we later extended this experiment to S100A12 and S100A7.[44, 45] This metal-depletion assay delineates which transition metals a protein binds with sufficiently high affinity such that the metals remain bound to the protein during a spin filtration step. To obtain preliminary insights into the metal-sequestering repertoire of mCP, we evaluated the ability of mCP and mCP-Ser to deplete metal ions from the Tris:TSB AMA medium in the absence and presence of a ≈2 mM Ca(II) supplement. This Ca(II) concentration mimics extracellular Ca(II) levels.[46] Because the analytical SEC experiments detailed above indicated that mCP requires >200 equivalents of Ca(II) to fully convert to the heterotetramer (Figure 3), we attempted to investigate metal depletion in the presence of 5 mM Ca(II) ions, but supplementation of Tris:TSB with this concentration of Ca(II) ions resulted in precipitation that confounded the analyses. We also evaluated the consequences of a ≈3 mM BME supplement because this reducing agent has been employed in antimicrobial activity assays with hCP,[7, 10, 23, 24] and it enhances the ability of hCP-Ser to deplete Fe from microbial growth medium.[31, 47]

The Tris:TSB medium employed in this work contained ≈3 μM Zn, ≈1.6 μM Fe, ≈0.5 μM Ni, and less than 150 nM of Mn, Co, and Cu. Treatment of Tris:TSB medium with 250 μg/mL (≈11 μM) mCP or mCP-Ser resulted in depletion of Mn, Fe, Ni, Cu and Zn comparable to that observed for 250 μg/mL hCP-Ser (Figure 4, Table S4). For Mn and Zn, only trace quantities were observed in the treated medium regardless of supplementation, These Mn and Zn depletion profiles were expected for several reasons: (i) mCP is accepted to participate in withholding Mn(II) and Zn(II), which requires high-affinity binding of these metal ions; (ii) the concentration of mCP employed in this assay exceeds the total concentration of metal ions in the Tris:TSB medium; and (iii) we previously observed that 250 μg/mL hCP-Ser fully depletes Mn and Zn from Tris:TSB medium with and without Ca(II) and BME supplements.[31] The proteins also depleted Fe from the Tris:TSB medium, especially in the presence of the Ca(II) and BME supplements, albeit to a lesser degree than observed for Mn and Zn. These results are consistent with our prior studies of Fe depletion by hCP-Ser, which demonstrated that maximum Fe depletion occurs in the presence of Ca(II) ions and BME, and illuminated that the His_6 site of hCP-Ser binds Fe(II) with high

affinity.[31] Depletion of Cu was also observed for all proteins, and the Ca(II) and BME supplements also afforded a slight enhancement of the depletion of this metal ion, an observation that warrants future investigation. Depletion of Ni also occurred under all examined conditions. Although no Co depletion was observed, we reason that this result reflects the low Co content (≈30 nM) of the growth medium as well as the expected thermodynamic preference of mCP for Zn(II) over Co(II). We previously reported that hCP-Ser readily binds Co(II) at both the His_3Asp and His_6 sites and that Zn(II) is thermodynamically favored at both sites,[23] and we expect that mCP will exhibit similar Co(II)-binding properties.

These metal-depletion data indicate that mCP has the propensity to chelate a number of first-row transition metal ions with sufficient affinity to retain the bound metal during spin filtration, suggesting that this protein has the capacity to withhold these nutrients from micoorganisms. Moreover, depletion of Fe, and also Cu, by mCP and mCP-Ser is enhanced by the presence of both BME and Ca(II) ions. This result may stem from a combination of an increase in transition metal affinities in the presence of excess Ca(II) ions (as observed for hCP) and redox speciation of the metal ions that is altered by the presence of a reducing agent to favor high-affinity binding (i.e. Fe(II) vs. Fe(III), as also observed for hCP). Future coordination chemistry studies of mCP will address these possibilities. Taken together, these data provide a foundation for elucidating the biological coordination chemistry of mCP and motivation for examining metals beyond Mn(II) and Zn(II) in future work.

mCP Exhibits Antimicrobial Activity

To provide a preliminary evaluation of the antimicrobial activity of mCP, we screened the protein (0–1000 μg/mL, 0–43 μM) against six bacterial strains that included two Gram-negative pathogens (*E. coli* CFT073 and *A. baumannii* ATCC 17961), three Gram-positive pathogens (*S. aureus* USA300 JE2, *S. epidermidis,* and *L. monocytogenes*), and the Gram-positive probiotic *L. plantarum* WCFS1 (Table S5). We examined the growth inhibitory activity of mCP and mCP-Ser at 37 °C in AMA medium preparations that contained 68% Tris buffer and 32% growth medium (TSB, BHI or MRS depending on the strain, Table S5) in the absence and presence of a ≈2-mM Ca(II) supplement, which mimics extracellular Ca(II) levels.[46]

We monitored growth at 8-h (Figure 5) and 20-h (Figure S4) timepoints, and focus this analysis on the former dataset. Overall, mCP inhibited the growth of these six bacterial strains to varying degrees (Figures 5A, S4A). The ≈2-mM Ca(II) supplement afforded enhanced growth inhibition against *E. coli* CFT073 (8-h time point only), *A. baumannii* 17961, *L. plantarum* WCSF1, and to a lesser extent, *L. monocytogenes*. On the basis of the 8-h time point, two Gram-positive strains, *S. epidermidis* NRS101 and *L. monocytogenes* 19115, appear to be most susceptible to mCP because complete or almost complete growth inhibition occurred at 250 μg/mL mCP regardless of Ca(II) supplementation. mCP-Ser also exhibited antibacterial activity (Figures 5B, S4B). A comparison of the data for mCP and mCP-Ser affords several observations about the relative antimicrobial activity of these proteins: (i) in the absence of Ca(II), mCP-Ser generally displays lower growth inhibitory activity than mCP, and (ii) the Ca(II)-induced enhancement of growth inhibitory activity is

greater for mCP-Ser than for mCP, and (iii) several strains exhibit growth recovery at the 20-h timepoint when treated with mCP-Ser. These trends are especially pronounced for *S. epidermidis* NRS101, *L. monocytogenes* ATCC 19115, and *L. plantarum* WCSF1. These results may be a consequence of differing protein stability where one or more of the Cys→Ser mutations in the apo mCP-Ser heterodimer destabilize the protein relative to mCP and binding of Ca(II) ions is compensatory. It is also possible that mCP-Ser possesses lower transition metal affinities than mCP in the absence of Ca(II), which would account for the lower antibacterial activity. Thus, we believe this initial study indicates that caution must be taken when employing mCP-Ser as a surrogate for the native protein. Prior studies of hCP and hCP-Ser reported that the Cys→Ser mutations have negligible effect on the growth inhibitory activity of the protein.[23]

Discussion

In this work, we report the purification and biochemical characterization of mCP, which provides a foundation for further studies of this protein. mCP can be readily obtained following overexpression of the mS100A8 and mS100A9 subunits in *E. coli* and reconstitution of the apo heterodimer, and in yields that will enable future biophysical and spectroscopic investigations of the protein. Preliminary characterization of mCP revealed that it has many comparable attributes to the human orthologue. Similar to hCP, Ca(II) ion binding causes two mCP heterodimers to self-associate and form a heterotetramer (Figure 3) and increases the stability of the protein to thermal denaturation (Figure S3). An initial evaluation of metal chelation by mCP demonstrates that it has the capacity to deplete multiple first-row transition metals ions – Mn, Fe, Ni, Cu, and Zn – from microbial growth medium, which is reminiscent of hCP (Figure 4). Moreover, this observation is in agreement with prior animal studies of infection, which indicate that mCP competes with microbes for Mn and Zn, as well as Cu.[7–10, 18] These data also suggest that mCP, like hCP, may contribute to the homeostasis of nutrient metals like Fe and Ni.[31, 35, 47] On the basis of the antibacterial activity assays presented in this work (Figure 5), mCP appears to have broad-spectrum growth inhibitory activity. Both the metal-depletion and antibacterial activity assays indicate that Ca(II) ions modulate the functional properties of mCP, enhancing transition metal affinities and growth inhibitory activity. These features are also reminiscent of hCP, and our prior investigations of hCP revealed that excess Ca(II) ions modulate its affinities for transition metal ions and antibacterial activity.[23, 30, 31]

This work also indicates some clear differences in the behavior of hCP and mCP that require further investigation as well as consideration in future experimental design and data interpretation. In particular, the current work reveals that, despite homology between the Ca(II)-binding loops in the S100A8 and S100A9 subunits of the human and murine polypeptides (Figure 1), mCP requires more equivalents of excess Ca(II) ions to fully tetramerize. The source of this disparity, and whether this decreased Ca(II) sensitivity has biological implications, is currently unknown and warrants examination. Extracellular Ca(II) ion concentrations are ≈2 mM,[46] and this work suggests that >200 equivalents of Ca(II) ions are required to fully tetramerize mCP. Thus, it is possible that full conversion to the heterotetramer is impaired at extracellular sites where the [Ca(II)]/[mCP] ratio is relatively

low because mCP is abundant. We expect that further biophysical studies of mCP as well as *ex vivo* analyses of murine specimens will shed light on this matter.

We also examined the cysteine-null variant mCP-Ser. Because the hCP-Ser variant has been employed extensively in studies of the human orthologue,[21–23] we reasoned that mCP-Ser could have comparable utility. Whereas both hS100A8 and mS100A8 have only one cysteine residue, which is conserved and located at position 42, the number and distribution of cysteine residues in the hS100A9 and mS100A9 differ. The human polypeptide contains only one cysteine at position 3, located two residues before an alternative translation start site defined by Met5. Neither Cys3 nor Met5 are found in mS100A9. Rather, the murine polypeptide has three cysteine residues at positions 80, 91 and 111. mCP-Ser exhibited similar Ca(II)-dependent tetramerization and metal-depletion profiles to mCP. However, we routinely obtained lower yields of mCP-Ser from folding, observed that its stability to thermal denaturation was reduced, and found differences between mCP and mCP-Ser in the antibacterial assays where mCP-Ser often exhibited lower antibacterial activity and greater Ca(II) dependence than mCP (Figures 5, S4). Together, these observations indicate that one or more of the Cys→Ser mutations in mCP-Ser destabilize the protein and compromise its function to some degree.

In closing, mCP has played and will continue to play a prominent role in studies of the host response to microbial infection. The purification and biochemical characterization presented in this work provides a foundation for continued elucidation of the biological coordination chemistry of mCP and other biochemical investigations at the host/microbe interface. In particular, we anticipate that biochemical and biophysical evaluation of mCP will provide additional molecular level insights into current working models and metal withholding by the murine innate immune system.

Supplementary Material

Refer to Web version on PubMed Central for supplementary material.

Acknowledgments

We thank Dr. M. B. Brophy for preliminary studies of mCP. We gratefully acknowledge the NSF (CHE-1352132) and NIH (R01GM118695) for financial support. R. C. Hadley is a recipient of a R. R. Schrock Summer Fellowship. The ICP-MS instrument is housed in the MIT Center for Environmental Health Sciences Bioanalytical Core supported by NIH grant P30-ES002109. The MIT Biophysical Instrumentation Facility for the Study of Complex Macromolecular Systems is supported by NSF grant 0070319. The staphylococcal strains were obtained from the Network on Antimicrobial Resistance in *Staphylococcus aureus* (NARSA) program supported under NIAID/NIH contract no. HHSN272200700055C.

Abbreviations

AMA	antimicrobial activity
BHI	brain heart infusion medium
BME	β-mercaptoethanol
CP	calprotectin

hCP	human calprotectin (including hCP-Ser, the Cys→Ser variant)
mCP	murine calprotectin (including mCP-Ser, the Cys→Ser variant)
DTT	dithiothreitol
Gu-HCl	guanidinium hydrochloride
HEPES	4-(2-hydroxyethyl)-1-piperazineethanesulfonic acid
ICP-MS	inductive-coupled plasma mass spectrometry
IPTG	isopropyl β-D-1-thiogalactopyranoside
LB	Luria-Bertani medium
LC-MS	liquid chromatography mass spectrometry
MES	2-(*N*-morpholino)ethanesulfonic acid
MRS	De Man, Rogosa, and Sharpe medium
PMSF	phenylmethylsulfonylfluroide
SEC	size exclusion chromatorgaphy
TCEP	tris(2-carboxyethyl)phosphine
TSB	tryptic soy broth medium

References

1. Zimmer DB, Eubanks JO, Ramakrishnan D, Criscitiello MF. Evolution of the S100 family of calcium sensor proteins. Cell Calcium. 2013; 53:170–179. [PubMed: 23246155]
2. Gifford JL, Walsh MP, Vogel HJ. Structures and metal-ion-binding properties of the Ca^{2+}-binding helix-loop-helix EF-hand motifs. Biochem J. 2007; 405:199–221. [PubMed: 17590154]
3. Zackular JP, Chazin WJ, Skaar EP. Nutritional immunity: S100 proteins at the host-pathogen interface. J Biol Chem. 2015; 290:18991–18998. [PubMed: 26055713]
4. Cunden LS, Nolan EM. Bioinorganic explorations of Zn(II) sequestration by human S100 host-defense proteins. Biochemistry. 2018; 57:1673–1680. [PubMed: 29381858]
5. Zygiel EM, Nolan EM. Transition metal sequestration by host-defense protein calprotectin. Ann Rev Biochem. 2018 in press.
6. Hobbs JAR, May R, Tanousis K, McNeill E, Mathies M, Gebhardt C, Henderson R, Robinson MJ, Hogg N. Myeloid cell function in MRP-14 (S100A9) null mice. Mol Cell Biol. 2003; 23:2564–2576. [PubMed: 12640137]
7. Corbin BD, Seeley EH, Raab A, Feldmann J, Miller MR, Torres VJ, Anderson KL, Dattilo BM, Dunman PM, Gerads R, Caprioli RM, Nacken W, Chazin WJ, Skaar EP. Metal chelation and inhibition of bacterial growth in tissue abscesses. Science. 2008; 319:962–965. [PubMed: 18276893]
8. Liu JZ, Jellbauer S, Poe AJ, Ton V, Pesciaroli M, Kehl-Fie TE, Restrepo NA, Hosking MP, Edwards RA, Battistoni A, Pasquali P, Lane TE, Chazin WJ, Vogl T, Roth J, Skaar EP, Raffatellu M. Zinc sequestration by the neutrophil protein calprotectin enhances *Salmonella* growth in the inflamed gut. Cell Host Microbe. 2012; 11:227–239. [PubMed: 22423963]
9. Diaz-Ochoa VE, Lam D, Lee CS, Klaus S, Behnsen J, Liu JZ, Chim N, Nuccio SP, Rathi SG, Mastroianni JR, Edwards RA, Jacobo CM, Cerasi M, Battistoni A, Ouellette AJ, Goulding CW,

Chazin WJ, Skaar EP, Raffatellu M. *Salmonella* mitigates oxidative stress and thrives in the inflamed gut by evading calprotectin-mediated manganese sequestration. Cell Host Microbe. 2016; 19:814–825. [PubMed: 27281571]

10. Hood MI, Mortensen BL, Moore JL, Zhang Y, Kehl-Fie TE, Sugitani N, Chazin WJ, Caprioli RM, Skaar EP. Identification of an *Acinetobacter baumannii* zinc acquisition system that facilitates resistance to calprotectin-mediated zinc sequestration. PLoS Pathog. 2012; 8:e1003068. [PubMed: 23236280]
11. Mortensen BL, Rathi S, Chazin WJ, Skaar EP. *Acinetobacter baumannii* response to host-mediated zinc limitation requires the transcriptional regulator Zur. J Bacteriol. 2014; 196:2616–2626. [PubMed: 24816603]
12. Juttukonda LJ, Chazin WJ, Skaar EP. *Acinetobacter baumannii* coordinates urea metabolism with metal import to resist host-mediated metal limitation. mBio. 2016; 7:e01475–01416. [PubMed: 27677795]
13. Nairn BL, Lonergan ZR, Wang J, Braymer JJ, Zhang Y, Calcutt MW, Lisher JP, Gilston BA, Chazin WJ, de Crecy-Lagard V, Giedroc DP, Skaar EP. The response of *Acinetobacter baumannii* to zinc starvation. Cell Host Microbe. 2016; 19:826–836. [PubMed: 27281572]
14. Achouiti A, Vogl T, Endeman H, Mortensen BL, Laterre PF, Wittebole X, van Zoelen MA, Zhang Y, Hoogerwerf JJ, Florquin S, Schultz MJ, Grutters JC, Biesma DH, Roth J, Skaar EP, van 't Veer C, de Vos AF, van der Poll T. Myeloid-related protein-8/14 facilitates bacterial growth during pneumococcal pneumonia. Thorax. 2014; 69:1034–1042. [PubMed: 25179663]
15. Gaddy JA, Radin JN, Loh JT, Piazuelo MB, Kehl-Fie TE, Delgado AG, Ilca FT, Peek RM, Cover TL, Chazin WJ, Skaar EP, Scott Algood HM. The host protein calprotectin modulates the *Helicobacter pylori cag* type IV secretion system via zinc sequestration. PLoS Pathog. 2014; 10:e1004450. [PubMed: 25330071]
16. Clark HL, Jhingran A, Sun Y, Vareechon C, de Jesus Carrion S, Skaar EP, Chazin WJ, Calera JA, Hohl TM, Pearlman E. Zinc and manganese chelation by neutrophil S100A8/A9 (calprotectin) limits extracellular *Aspergillus fumigatus* hyphal growth and corneal infection. J Immunol. 2016; 196:336–344. [PubMed: 26582948]
17. Urban CF, Ermert D, Schmid M, Abu-Abed U, Goosmann C, Nacken W, Brinkmann V, Jungblut PR, Zychlinsky A. Neutrophil extracellular traps contain calprotectin, a cytosolic protein complex involved in host defense against *Candida albicans*. PLoS Pathog. 2009; 5:e1000639. [PubMed: 19876394]
18. Besold AN, Gilston BA, Radin JN, Ramsoomair C, Culbertson EM, Li CX, Cormack BP, Chazin WJ, Kehl-Fie TE, Culotta VC. Role of calprotectin in withholding zinc and copper from *Candida albicans*. Infect Immun. 2017; 86:e00779–00717.
19. Juttukonda LJ, Berends ETM, Zackular JP, Moore JL, Stier MT, Zhang Y, Schmitz JE, Beavers WN, Wijers CD, Gilston BA, Kehl-Fie TE, Atkinson J, Washington MK, Peebles RS, Chazin WJ, Torres VJ, Caprioli RM, Skaar EP. Dietary manganese promotes Staphylococcal infection of the heart. Cell Host Microbe. 2017; 22:531–542. [PubMed: 28943329]
20. Wakeman CA, Moore JL, Noto MJ, Zhang Y, Singleton MD, Prentice BM, Gilston BA, Doster RS, Gaddy JA, Chazin WJ, Caprioli RM, Skaar EP. The innate immune protein calprotectin promotes *Pseudomonas aeruginosa* and *Staphylococcus aureus* interaction. Nat Commun. 2016; 7:11951. [PubMed: 27301800]
21. Korndörfer IP, Brueckner F, Skerra A. The crystal structure of the human $(S100A8/S100A9)_2$ heterotetramer, calprotectin, illustrates how conformational changes of interacting α-helices can determine specific association of two EF-hand proteins. J Mol Biol. 2007; 370:887–898. [PubMed: 17553524]
22. Hunter MJ, Chazin WJ. High level expression and dimer characterization of the S100 EF-hand proteins, migration inhibitory factor-related proteins 8 and 14. J Biol Chem. 1998; 273:12427–12435. [PubMed: 9575199]
23. Brophy MB, Hayden JA, Nolan EM. Calcium ion gradients modulate the zinc affinity and antibacterial activity of human calprotectin. J Am Chem Soc. 2012; 134:18089–18100. [PubMed: 23082970]
24. Damo SM, Kehl-Fie TE, Sugitani N, Holt ME, Rathi S, Murphy WJ, Zhang Y, Betz C, Hench L, Fritz G, Skaar EP, Chazin WJ. Molecular basis for manganese sequestration by calprotectin and

roles in the innate immune response to invading bacterial pathogens. Proc Natl Acad Sci. 2013; 110:3841–3846. [PubMed: 23431180]

25. Gagnon DM, Brophy MB, Bowman SE, Stich TA, Drennan CL, Britt RD, Nolan EM. Manganese binding properties of human calprotectin under conditions of high and low calcium: X-ray crystallographic and advanced electron paramagnetic resonance spectroscopic analysis. J Am Chem Soc. 2015; 137:3004–3016. [PubMed: 25597447]
26. Vogl T, Roth J, Sorg C, Hillenkamp F, Strupat K. Calcium-induced noncovalently linked tetramers of MRP8 and MRP14 detected by ultraviolet matrix-assisted laser desorption/ionization mass spectrometry. J Am Soc Mass Spectrom. 1999; 10:1124–1130. [PubMed: 10536818]
27. Strupat K, Rogniaux H, Van Dorsselaer A, Roth J, Vogl T. Calcium-induced noncovalently linked tetramers of MRP8 and MRP14 are confirmed by electrospray ionization-mass analysis. J Am Soc Mass Spectrom. 2000; 11:780–788. [PubMed: 10976885]
28. Vogl T, Leukert N, Barczyk K, Strupat K, Roth J. Biophysical characterization of S100A8 and S100A9 in the absence and presence of bivalent cations. Biochim Biophys Acta. 2006; 1763:1298–1306. [PubMed: 17050004]
29. Stephan JR, Nolan EM. Calcium-induced tetramerization and zinc chelation shield human calprotectin from degradation by host and bacterial extracellular proteases. Chem Sci. 2016; 7:1962–1975. [PubMed: 26925211]
30. Hayden JA, Brophy MB, Cunden LS, Nolan EM. High-affinity manganese coordination by human calprotectin is calcium-dependent and requires the histidine-rich site formed at the dimer interface. J Am Chem Soc. 2013; 135:775–787. [PubMed: 23276281]
31. Nakashige TG, Zhang B, Krebs C, Nolan EM. Human calprotectin is an iron-sequestering host-defense protein. Nat Chem Biol. 2015; 11:765–771. [PubMed: 26302479]
32. Sohnle PG, Collins-Lech C, Wiessner JH. Antimicrobial activity of an abundant calcium-binding protein in the cytoplasm of human neutrophils. J Infect Dis. 1991; 163:187–192. [PubMed: 1984467]
33. Sohnle PG, Collins-Lech C, Wiessner JH. The zinc-reversible antimicrobial activity of neutrophil lysates and abscess fluid supernatants. J Infect Dis. 1991; 164:137–142. [PubMed: 2056200]
34. Clohessy PA, Golden BE. Calprotectin-mediated zinc chelation as a biostatic mechanism in host-defense. Scand J Immunol. 1995; 42:551–556. [PubMed: 7481561]
35. Nakashige TG, Zygiel EM, Drennan CL, Nolan EM. Nickel sequestration by the host-defense protein human calprotectin. J Am Chem Soc. 2017; 139:8828–8836. [PubMed: 28573847]
36. Raftery MJ, Geczy CL. Identification of noncovalent dimeric complexes of the recombinant murine S100 protein CP10 by electrospray ionization mass spectrometry and chemical cross-linking. J Am Soc Mass Spectrom. 1998; 9:533–539. [PubMed: 9879368]
37. Raftery MJ, Collinson L, Geczy CL. Overexpression, oxidative refolding, and zinc binding of recombinant forms of the murine S100 protein MRP14 (S100A9). Protein Expr Purif. 1999; 15:228–235. [PubMed: 10049680]
38. Lackmann M, Cornish CJ, Simpson RJ, Moritz RL, Geczy CL. Purification and structural analysis of a murine chemotactic cytokine (CP-10) with sequence homology to S100 proteins. J Biol Chem. 1992; 267:7499–7504. [PubMed: 1559987]
39. Raftery MJ, Harrison CA, Alewood P, Jones A, Geczy CL. Isolation of the murine S100 protein MRP14 (14 kDa migration-inhibitory-factor-related protein) from activated spleen cells: characterization of post-translational modifications and zinc binding. Biochem J. 1996; 316:285–293. [PubMed: 8645219]
40. Kocher M, Kenny PA, Farram E, Abdul Majid KB, Finlay-Jones JJ, Geczy CL. Functional chemotactic factor CP-10 and MRP-14 are abundant in murine abscesses. Infect Immun. 1996; 64:1342–1350. [PubMed: 8606099]
41. Mestas J, Hughes CCW. Of mice and not men: differences between mouse and human immunology. J Immunol. 2004; 172:2731–2738. [PubMed: 14978070]
42. Brophy MB, Nakashige TG, Gaillard A, Nolan EM. Contributions of the S100A9 C-terminal tail to high-affinity Mn(II) chelation by the host-defense protein human calprotectin. J Am Chem Soc. 2013; 135:17804–17817. [PubMed: 24245608]

43. Nakashige TG, Stephan JR, Cunden LS, Brophy MB, Wommack AJ, Keegan BC, Shearer JM, Nolan EM. The hexahistidine motif of host-defense protein human calprotectin contributes to zinc withholding and its functional versatility. J Am Chem Soc. 2016; 138:12243–12251. [PubMed: 27541598]

44. Cunden LS, Gaillard A, Nolan EM. Calcium ions tune the zinc-sequestering properties and antimicrobial activity of human S100A12. Chem Sci. 2016; 7:1338–1348. [PubMed: 26913170]

45. Cunden LS, Brophy MB, Rodriguez GE, Flaxman HA, Nolan EM. Biochemical and functional evaluation of the intramolecular disulfide bonds in the zinc-chelating antimicrobial protein human S100A7 (Psoriasin). Biochemistry. 2017; 56:5726–5738. [PubMed: 28976190]

46. Brini M, Ottolini D, Cali T, Carafoli E. Calcium in health and disease. Met Ions Life Sci. 2013; 13:81–137. [PubMed: 24470090]

47. Nakashige TG, Nolan EM. Human calprotectin affects the redox speciation of iron. Metallomics. 2017; 9:1086–1095. [PubMed: 28561859]

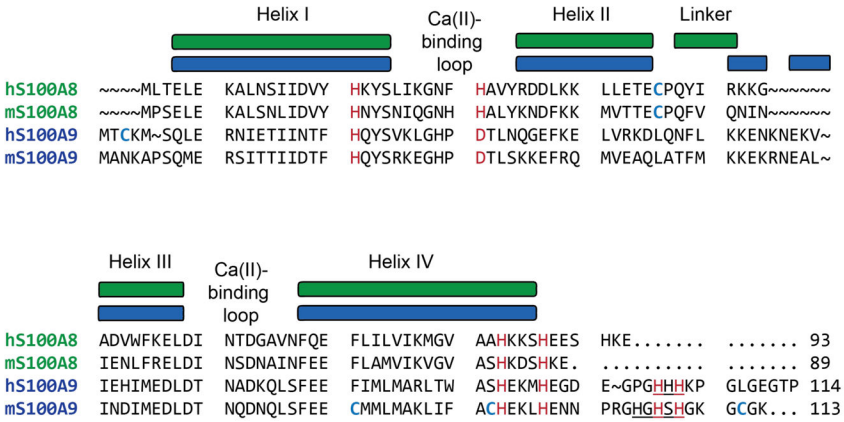

Figure 1.

Amino acid sequence alignment of the S100A8 and S100A9 subunits of human (h) and murine (m) CP. Metal-binding residues of the human polypeptides and conserved murine residues are highlighted in red. Cys residues for all proteins are bolded and in blue. The C-terminal HHH and HxHxH motifs in the human and murine S100A9 subunits are underlined. The depictions of secondary structure are for the human orthologues.

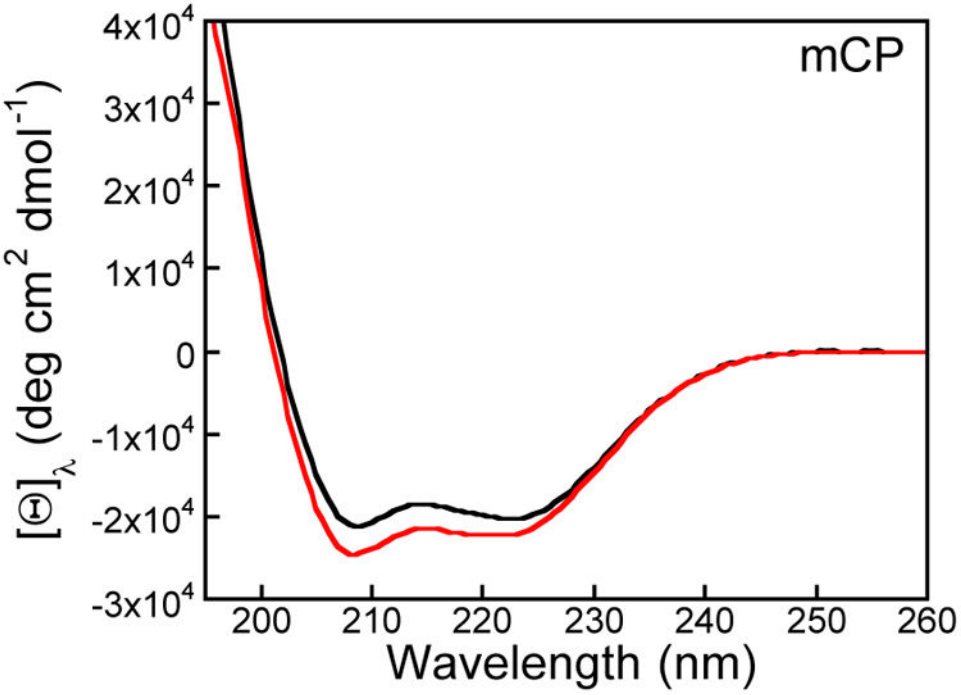

Figure 2.

CD spectra of mCP in the absence (black) and presence (red) of 2 mM Ca(II) (1 mM Tris-HCl, pH 7.5, 25 °C). The CD spectra of mCP-Ser are presented in Figure S2.

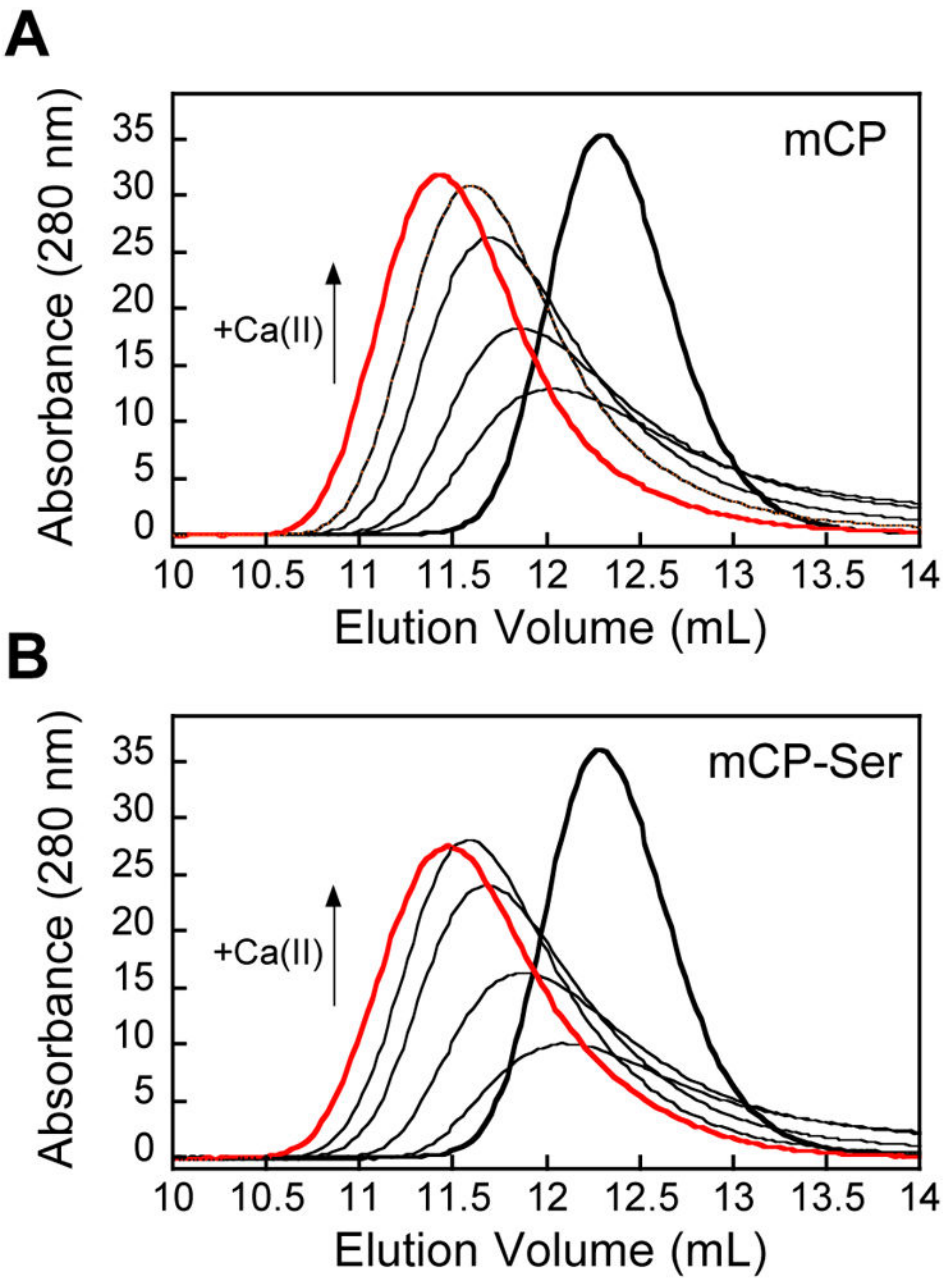

Figure 3.

mCP displays Ca(II)-dependent heterotetramer formation. Analytical SEC chromatograms of 100 μM mCP in the absence (thick black trace) and presence of 1, 2, 5, 10, and 25 mM (thick red trace) Ca(II) (75 mM HEPES, 100 mM NaCl, pH 7.0, 200 μM TCEP) at 4 °C. Elution volumes and corresponding molecular weights are given in Table S3.

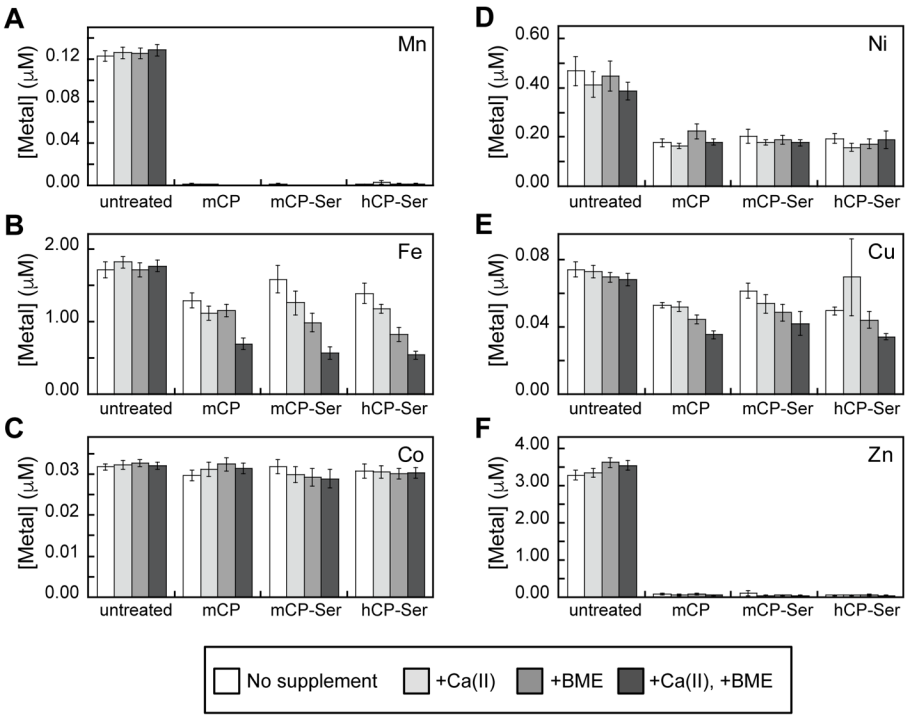

Figure 4.

mCP depletes transition metal ions from Tris:TSB medium. (A) Mn depletion; (B) Fe depletion; (C) Co depletion; (D) Ni depletion; (E) Cu depletion; (F) Zn depletion. The medium was incubated with 250 μg/mL mCP, mCP-Ser, or hCP-Ser (20 h, 30 °C). Proteins were removed by spin filtration and the metal content of the filtrate was measured by ICP-MS (mean ± SEM, $n \geq 4$). The Tris:TSB medium contained no supplement (white bars), a 2-mM Ca(II) supplement (light grey bars), a 3-mM BME supplement (medium grey bars), or both 2-mM Ca(II) and 3-mM BME supplements (dark grey bars). Raw ICP-MS data are provided in Table S4.

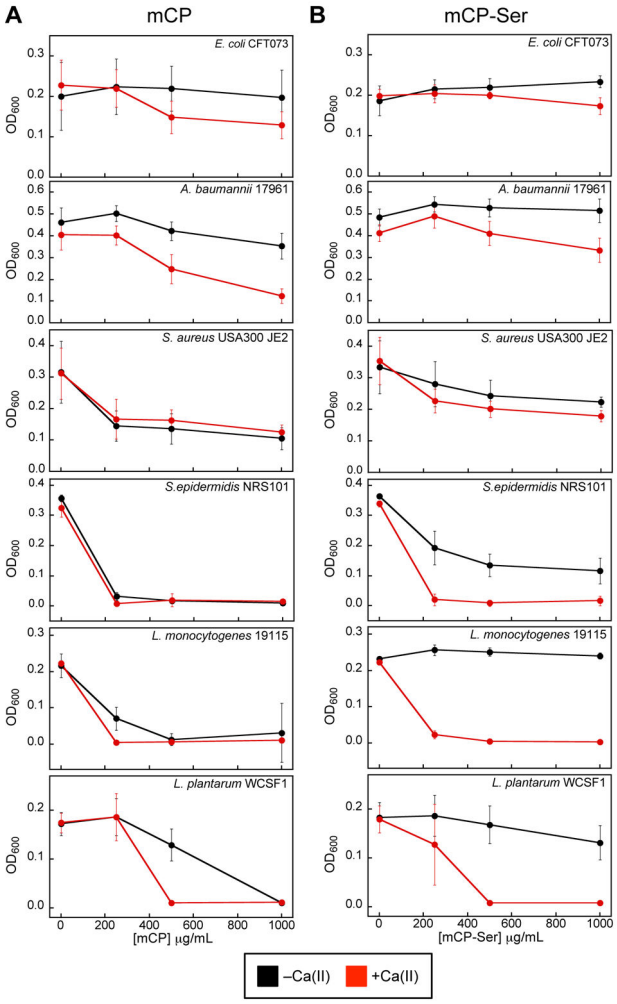

Figure 5.

mCP inhibits growth of various bacterial species. (A) Growth inhibitory activity of mCP. (B) Growth inhibitory activity of mCP-Ser. Both proteins were assayed in the absence (black) and presence (red) of a 2-mM Ca(II) supplement in the AMA medium (Tris:TSB, T = 37 °C, 8 h) (mean ± SDM, $n \geq 3$). Figure S4 contains data from the same assay at a 20-h time point.